Observation of photoinduced intersubband transitions in one-dimensional semiconductor quantum wires

S. Calderon, O. Kadar, and A. Sa'ar*
Department of Applied Physics, The Hebrew University of Jerusalem, Jerusalem 91904, Israel

A. Rudra, E. Martinet, K. Leifer, and E. Kapon
Department of Physics, Ecole Polytechnique Federal de Lausanne, CH-1015 Lausanne, Switzerland
(Received 11 April 2000; revised manuscript received 6 June 2000)

We report on midinfrared intersubband transitions between the quantized levels of undoped $GaAs/Al_xGa_{1-x}As$ quantum wires that are grown on nonplanar substrates. Using photoinduced infrared absorption spectroscopy, we were able to resolve two absorption lines in the 120–160 meV range. The first absorption line follows the polarization selection rules for intersubband transitions and exhibits photoinduced excitation profile that resembles the photoluminescence excitation spectrum of the quantum wires. The second absorption resonance, at a higher energy, is not polarized and resembles the photoluminescence spectrum of the side quantum wells. Based on these results and energy level calculations, we assign the first absorption resonance to intersubband transition between the quantized subbands of the quantum wires. The origin of the second resonance is less clear. We propose a model that attributes this resonance to an interface localized exciton mode that arises from interface roughness of the side quantum wells and the wires.

Intersubband optical transitions between the quantized levels of low-dimensional (low-*D*) semiconductor structures provide a very powerful experimental tool for studying fundamental properties of these nanostructures.[1] In two-dimensional (2D) semiconductor structures (e.g., quantum wells) intersubband transitions (IST's) were utilized also for developing new classes of midinfrared optoelectronic devices such as photodetectors,[1,2] modulators,[3] and recently also lasers.[4] These transitions provide a direct way to probe the energy quantization in either the conduction or the valence band, the shape, and the symmetry of the envelope wave functions involved in the transitions. Intersubband spectroscopy was also utilized to zero-dimensional quantum dot (QD) structures.[5–8] In contrast to quantum wells, the additional confinement of the charged carriers changes the IST polarization selection rules that could be important for normal-incident photodetection applications.[8,9] Furthermore, theoretical works[10,11] predict slower relaxation processes in low-D structures due to the reduced electron-phonon interaction that could dramatically improve the performances of intersubband photodetectors and lasers.

Previous works on IST's in low-D structures were carried out mainly on 2D structures where the additional confinement was achieved by the application of either magnetic or electric field. Examples include quantum dots and antidotes,[12] metal-oxide-semiconductor (MOS) inversion layers,[13] and resonant inelastic light scattering experiments.[14] More recently, IST's were observed in self-organized QD's grown by the Stranski-Krastanov mode of growth.[5–9] However, this system is characterized by a broad inhomogeneous distribution of QD sizes that screens many important features of low-D structures. In addition, the presence of a large residual strain in these QD's (Ref. 15) may lead to a wrong interpretation of the IST polarization selection rules since band mixing might be due to strain rather than size quantization.

In this paper we provide direct experimental evidences for intersubband optical transitions in one-dimensional (1D) quantum wire (QWR) structures. We have chosen to work with V-groove QWR's grown on nonplanar substrates that were demonstrated recently to show optical and electronic features that are directly related to the lower dimensionality of these structures.[16–18] Using photoinduced infrared absorption spectroscopy,[19] photoluminescence (PL), and photoluminescence excitation (PLE), we were able to resolve infrared absorption lines that are assigned with transitions between the quantized subbands of the QWR.

The sample used for the experiment was grown by low-pressure organometallic chemical vapor deposition on a semi-insulating (100) GaAs substrate, patterned along the $[01\bar{1}]$ direction. The grooves were fabricated by holographic photolithography followed by wet chemical etching with a groove periodicity of 0.5 μm. The structure consists of 55-nm-thick $Al_{0.32}Ga_{0.68}As$ buffer layer followed by ten periods of GaAs QWR's and a top 117-nm-thick $Al_{0.32}Ga_{0.68}As$ capped with 12-nm GaAs layer. Each period consists of a GaAs QWR with a nominal thickness of 2.6 nm and a 32-nm-thick $Al_{0.32}Ga_{0.68}As$ barrier.

Figure 1 shows dark field TEM cross section views of the sample. Figure 1(a) shows three grooves with the first few crescent-shaped QWR's near the bottom of the grooves. In Fig. 1(b) one can see a larger magnification of the QWR region. Notice that, due to sharpening of the groove during the $Al_xGa_{1-x}As$ layer growth and the higher growth rate of GaAs at the bottom of the groove, one obtains the well-known crescent-shape QWR profile.[16–18] Notice also the presence of GaAs-rich vertical QW's connecting the individual QWR's at the bottom of the groove. From this figure we find the thickness of the GaAs QWR, at the bottom of the groove, to be about 7.9 nm.

PL and PLE spectra of the sample at 8 K are shown in Fig. 2. The sample was mounted in a helium-flow cryostat

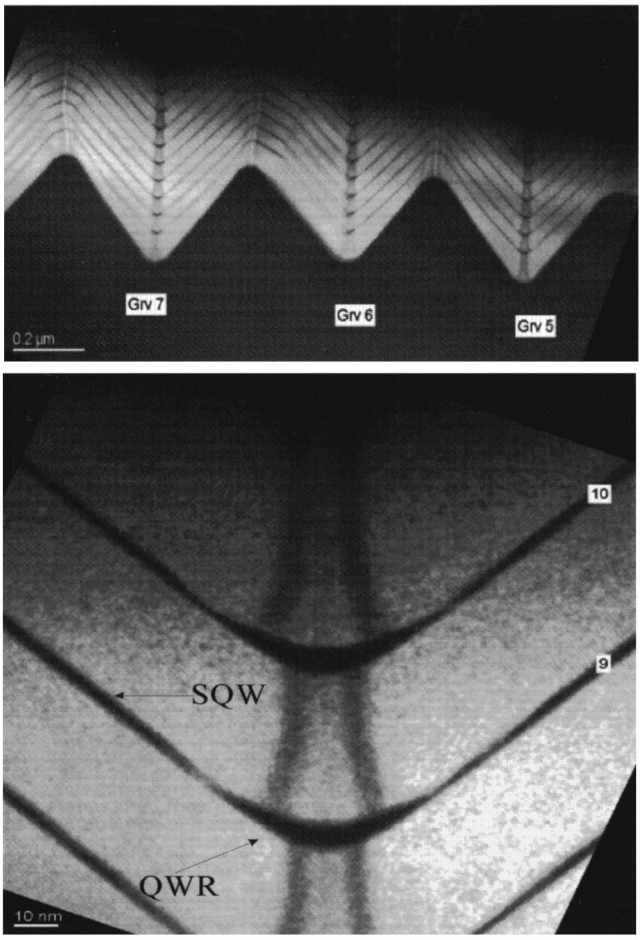

FIG. 1. TEM cross section micrograph of (a) an array of V-groove QWR's grown on top of a 0.5-μm grating; (b) a larger magnification of the QWR profile.

and the spectra were measured using a tunable Ti: sapphire laser operating either at 690 nm (PL) or at the range of 710–800 nm (PLE). A typical power of the pump laser was about 50 μW. The PL spectrum consists of three peaks at 1.591, 1.674, and 1.720 eV that are assigned with excitonic transitions from the QWR, the side QW's (SQW's), and the top QW's, respectively. The identification of these peaks is based on previous studies of similar structures using cathode-luminescence imaging that relates each peak to its spatial origin.[20] The excitonic origin of the various peaks was also confirmed by time resolved PL spectroscopy at high excitation levels.[21] For the PLE measurements, the probe was set to an energy of 1.591 eV that is related to the QWR PL line. The small Stockes shift, of about 6.4 meV, between the PL and the PLE onset and the narrow linewidth of the QWR peak [full width at half maximum (FWHM) of 11.2 meV] provides a clear indication to the high quality of the sample.

The PLE spectra reveal up to six peaks that correspond to excitonic transitions from higher subbands of the 1D QWR. The first five peaks appear at 1.600, 1.627, 1.659, 1.682, and 1.713 eV and are related to c_{1n}-h_{1n} transitions where h_{1n} stands for the nth mixed lateral subband of the holes (heavy and light holes, see Ref. 22) and c_{1n} stands for the nth lateral conduction subband.

For the infrared (IR) absorption measurements the two

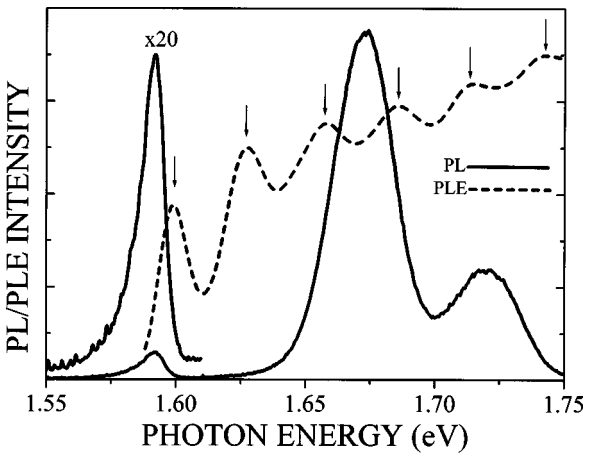

FIG. 2. Low-temperature (8 K) PL (solid line) and PLE (dashed line) spectra of the QWR sample. The arrows in the PLE spectrum indicate the excited electron-hole transitions in the QWR.

edges of a 5-mm-long bar of the sample were polished in a 45° angle to form a multipass waveguide geometry. We choose a sample geometry where the grooves are perpendicular to the waveguide direction so that the polarization of the IR beam can be set either along the wire axis (p polarization) or with a component along the growth direction (s polarization). A pump-probe technique, where a Ti:sapphire laser serves as a pump while an IR beam from a black-body source serves as a probe, was used. The IR beam was collected with a ZnSe lens into a $\frac{1}{8}$ m IR spectrometer and detected with a $Hg_xCd_{1-x}Te$ detector. By introducing a chopper operating at a frequency of 1.7 kHz either into the IR beam or into the pump beam and using a lock-in detection, we were able to measure the linear transmission T and the photoinduced transmission ΔT, respectively. Figure 3 shows two typical photoinduced absorption (PIA) spectra taken at 105 K (with $-\Delta T/T$ being proportional to the photoinduced absorption). In Fig. 3(a) the pump laser energy

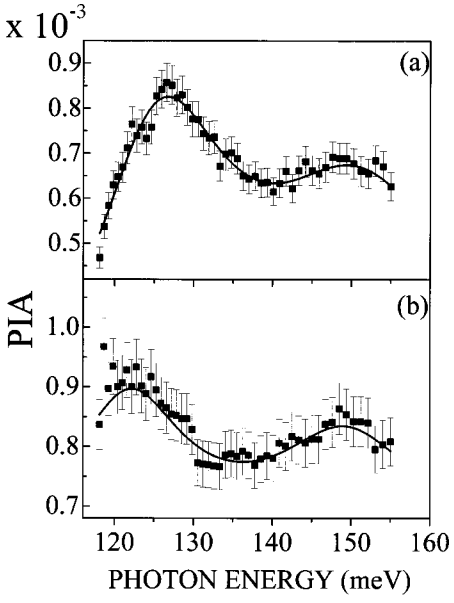

FIG. 3. Photoinduced absorption spectra at 105 K taken with the pump laser energy tuned to (a) 1.63 eV and (b) 1.67 eV.

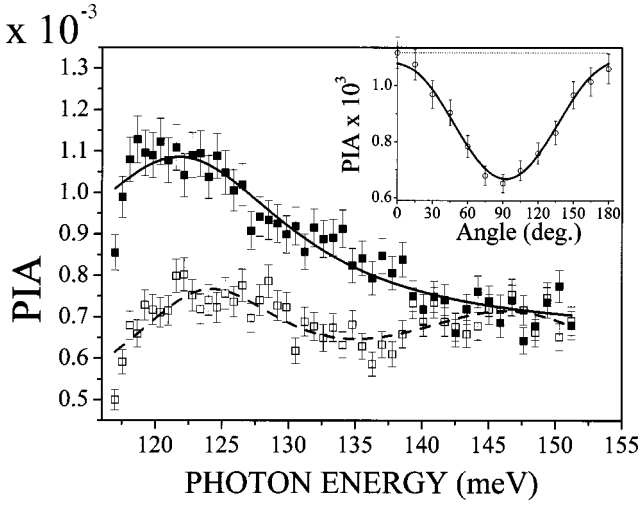

FIG. 4. Polarized photoinduced absorption spectra for *p* polarization (solid line) and *s* polarization (dashed line). The pump energy is 1.63 eV. The inset shows the intensity of the PIA line at 125 meV vs the polarization angle (symbols) and the fit to $\cos^2\phi$ (solid line).

was tuned to 1.630 eV (above the QWR line) while in Fig. 3(b) the pump energy was 1.670 eV (SQW). Two absorption lines at 125 and 148 meV, with a FWHM of about 10 meV, are clearly resolved. Notice that, when the pump energy is tuned to 1.630 eV, the PIA line at 125 meV is significantly stronger than the second PIA line at 148 meV. This should be compared to the case where the pump energy is tuned to the SQW line at 1.670 eV where both PIA lines are of the same order. In addition, we observe a small redshift (of about 2–3 meV) of the first PIA line when the pump laser beam is tuned to the SQW line at 1.670 eV. To resolve the origin of the PIA lines we introduced a polarizer to the optical pathlength of the IR beam and repeated the measurements for various polarization angles. Figure 4 shows two spectra, taken for *p* polarization (solid line) and for *s* polarization (dashed line). It can be seen that the first PIA line at 125 meV is preferentially polarized along the QWR plane as expected from IST's while the second line at 148 meV is not polarized. The inset to this figure shows that the 125 meV PIA line follows the $\cos^2\phi$ dependency (with ϕ being the polarization angle relative to the *p* polarization) with a modulation depth of about 0.26.

Further investigation of the PIA lines was done by measuring the PIA excitation spectra. In this experiment, the pump photon energy was tuned across the 1.55–1.72 eV range while the mid-IR probe beam was set either at the 125 or 148 meV PIA lines. Figure 5 shows the PIA excitation profiles for both cases for either the *p* polarization (allowed IST) and the *s* polarization (IST forbidden). When the IR probe is set to the 125 meV PIA line, the allowed polarization follows the PLE spectrum of the QWR. On the other hand, the forbidden IR polarization shows a stairlike profile with the first stair beginning at 1.58 eV and the second at 1.66 eV. Notice that these energies resemble the PL lines of the QWR and the SQW respectively. A similar profile is obtained when the IR probe is set to the 148 meV PIA line. However, here we find the excitation profile of the forbidden IR polarization to dominate over the excitation spectrum of the allowed IR polarization.

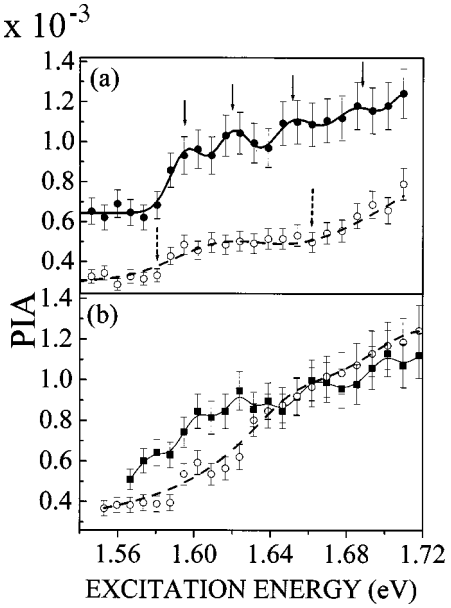

FIG. 5. PIA excitation spectra for *s* polarization (solid lines) and *p* polarization (dashed lines) taken with the probe energy set to (a) 125 meV and (b) 148 meV.

Let us now discuss the origin of the PIA lines. The PIA experiments involve excitation of electron-hole pairs that populate the ground excitonic state of our intentionally undoped structure. PIA signals are associated with excitation into higher states of our structure by the IR-probe beam. The first peak at 125 meV follows the selection rules of electronic intersubband transitions within the QWR.[23] This conclusion is supported by the observation that the 125 meV PIA line is mostly significant when the pump energy is in resonance with the QWR PL line. Furthermore, we found that the excitation profile of the 125-meV PIA line resembles the QWR PLE profile for the allowed IST polarization. Hence, all these data support our assignment of this transition being a photoinduced IST of the QWR. In order to assign this transition to specific subbands of the QWR one has to calculate the energy band structure of the QWR. Although an accurate model requires a solution of the eight-band $\mathbf{k}\cdot\mathbf{p}$ Hamiltonian, it has been shown recently[22] that energy spacing between valence subbands are of the order of 10 meV for a QWR of our size. Therefore, conduction intersubband transitions are most likely responsible for the observed PIA line. This has also been confirmed by calculating the energy spectrum of the conduction subbands and the 2D envelope wave functions using the local envelope state approach[24] and the TEM cross section image of Fig. 1. Taking into account a few monolayer fluctuations we found that the energy of the $(c_{11}\text{-}h_{11})\rightarrow(c_{21}\text{-}h_{11})$ IST is in the range 120–140 meV, in a reasonably good agreement with our PIA measurements. Furthermore, our calculations give, $(c_{12}\text{-}c_{11})\approx 20-25$ meV, in a good agreement with the results of the PLE and the PIA excitation spectra. We conclude that the first PIA line at 125 meV is related to a vertical IST into the first excited vertical subband while the excitation spectrum probes the first few lateral subbands of the QWR.

The origin of the second PIA transition is less clear and several explanations are possible. We would like to point out that a similar unpolarized PIA transition has been observed

in GaAs QW's and was assigned to an interface-localized exciton.[19,25] In QW's, however, it was found that the localized exciton PIA signal is much weaker than that of the QW exciton. Adopting this explanation and taking into account the filling factor ratio between the QWR exciton and the interface-localized exciton, which may arise from either the side QW's or roughness and monolayer fluctuations along the axis of the groove, one may expect both transitions to be of the same order of magnitude. Furthermore, monolayer fluctuations along the axis of the QWR are expected to release the intersubband selection rules as observed in our experiment. In addition, the localized exciton model can also explain the PIA excitation profile of the forbidden polarization. Once the pump energy is tuned to (and above) the SQW energy, the SQW interface-localized exciton mode is turned on and contributes to the excitation profile. Notice also that at the working temperature and the pump power level used in our experiment, it is very likely to assume that this exciton is rapidly ionized giving rise to an excitation profile of free electron-hole plasma as observed in our experiment. Despite that our interface-localized exciton model provides a reasonable explanation to the second PIA line, other explanations cannot be ruled out and additional experimental work is needed to explore the characteristics and the origin of this line.

In conclusion, photoinduced IST in undoped V-groove QWR were observed. Absorption spectroscopy revealed two PIA lines at 125 and 148 meV. The first PIA line follows the IST selection rules and is assigned with a transition between the ground and first excited subbands of the QWR conduction. The second PIA line does not follow the IST selection rules and has been assigned with interface-localized exciton mode of the various QW's of the structure.

*Corresponding author. E-mail address: saar@vms.huji.ac.il

[1] *Intersubband Transitions in Quantum Wells: Physics and Devices*, edited by S. S. Li and Y.-K. Su (Kluwer Academic, Boston, 1998), and references therein.

[2] B. F. Levine, J. Appl. Phys. **74**, R1 (1993).

[3] R. Kapon, N. Cohen, A. Sa'ar, V. Thierry-Mieg, and R. Planel, Appl. Phys. Lett. **75**, 1583 (1999).

[4] J. Faist, F. Capasso, D. Sivco, C. Cirtori, A. L. Hutchinson, S. N. G. Chu, and A. Y. Cho, Science **264**, 553 (1994); F. Capasso, C. Gmachl, D. Sivco, and A. Y. Cho, Phys. World **12**, 27 (1999).

[5] H. Drexler, D. Leonard, W. Hansen, J.-P. Kotthaus, and P.-M. Petroff, Phys. Rev. Lett. **73**, 1726 (1994).

[6] J. Phillips, K. Kamath, X. Zhou, N. Chervela, and P. Bhattachaya, Appl. Phys. Lett. **71**, 2079 (1997).

[7] S. Sauvage, P. Boucaud, F. H. Julien, J.-M. Gerard, and J.-Y. Marzin, J. Appl. Phys. **82**, 3396 (1997).

[8] A. Weber, O. Gauthier-Lafaye, F. H. Julien, J. Brault, M. Gendry, Y. Desieres, and T. Benyattou, Appl. Phys. Lett. **74**, 413 (1999).

[9] K. W. Berryman, S. Lyon, and M. Segev, Appl. Phys. Lett. **70**, 1861 (1997); D. Pan, E. Towe, and S. Kennerly, *ibid.* **73**, 1937 (1998).

[10] H. Benisty, C. M. Sotomayor-Torres, and C. Weisbuch, Phys. Rev. B **44**, 10 945 (1991).

[11] I. Vurgaftman, Y. Lam, and J. Singh, Phys. Rev. B **50**, 14 309 (1994).

[12] K. Bollweg, T. Kurth, D. Heitmann, V. Gudmundsson, E. Vasiliadou, P. Grambow, and K. Eberl, Phys. Rev. Lett. **76**, 2774 (1996).

[13] W. Hansen, M. Horst, J. P. Kotthaus, U. Merkt, Ch. Sikorski, and K. Ploog, Phys. Rev. Lett. **58**, 2586 (1987).

[14] A. R. Goni, A. Pinczuk, J. S. Weiner, J. M. Calleja, B. S. Dennis, L. N. Pfeiffer, and K. W. West, Phys. Rev. Lett. **67**, 3298 (1991).

[15] D. Bimberg, M. Grundman, and N. N. Ledenstov, MRS Bull. **23**, 31 (1998), and references therein.

[16] M. Walther, E. Kapon, J. Christen, D. M. Hwang, and R. Bhat, Appl. Phys. Lett. **60**, 521 (1991).

[17] A. Gustafsson, F. Reinhardt, G. Biasiol, and E. Kapon, Appl. Phys. Lett. **67**, 3673 (1995).

[18] F. Vouilloz, D. Y. Oberli, M.-A. Dupertuis, A. Gustafsson, F. Reinhardt, and E. Kapon, Phys. Rev. Lett. **78**, 1580 (1997).

[19] M. Olszakier, E. Ehrenfreund, E. Cohen, J. Bajaj, and G. J. Sullivan, Phys. Rev. Lett. **62**, 2997 (1989); Y. Garini *et al.*, Surf. Sci. **263**, 561 (1992).

[20] A. Gustafsson, L. Samuelson, D. Hessman, J.-O. Malm, G. Vermeire, and P. Demeester, J. Vac. Sci. Technol. B **13**, 308 (1995).

[21] R. Ambigapathy *et al.*, Phys. Rev. Lett. **78**, 3579 (1997).

[22] F. Vouilloz, D. Y. Oberli, M.-A. Dupertuis, A. Gustafsson, F. Reinhardt, and E. Kapon, Phys. Rev. B **57**, 12 378 (1998).

[23] The extension of the intersubband selection rules to 1D QWR structures can be explained as follows. Since IST's are related to transitions between envelope states that are polarized perpendicular to the QWR axis, all transition dipoles should be polarized perpendicular to this axis. This picture, however, ignores band-mixing corrections that are expected to be negligible for conduction electrons. See Ref. 24 for more details.

[24] A. Sa'ar, S. Calderon, A. Givant, O. Ben-Shalom, E. Kapon, and C. Caneau, Phys. Rev. B **54**, 2675 (1996).

[25] M. Olszakier, E. Ehrenfreund, E. Cohen, J. Bajaj, G. J. Sullivan, and D. Miller, Superlattices Microstruct. **5**, 283 (1989).